A meshfree method for the transverse vibration of strain gradient nanoplate with elastic boundary condition

Wang LI, *†Lifeng WANG, Jingnong JIANG

State Key Laboratory of Mechanics and Control of Mechanical Structures
Nanjing University of Aeronautics and Astronautics
Nanjing 210016, China

*Presenting author: walfe@nuaa.edu.cn
†Corresponding author: walfe@nuaa.edu.cn

Abstract

A meshfree method based on moving least square (MLS) approximation is used to study the vibration of the strain gradient plates. A high-order shifted and scaled polynomial basis is proposed to deal with the strain gradient elastic plates described by higher order differential equation. The natural frequencies of the strain gradient plates and classic Kirchhoff plates with elastically supported boundary are obtained by the MLS method. The natural frequencies of the strain gradient plates obtained by the meshfree method are in good agreement with the theoretical results for all boundaries simply supported case. Finally, the MLS method is used to study the vibration of the strain gradient plates with different boundary conditions and the nonlocal parameter which show the small scale effects.

Keywords: Shifted and scaled polynomial basis, MLS method, Strain gradient, Scale effect, Elastic boundary condition

Introduction

In micro or nano-scale, the classic continuum mechanics might be invalid to describe size effects due to the absence of additional material length scale parameters in constitutive laws. In 1960s, Toupin [1] and Mindlin [2][3] introduced high-order gradient terms into the classical constitutive relation. They established the strain gradient elastic theory, which can take the influence of the long range force and the effects microstructure into its constitutive relation. Papargyri-Beskou et al. [4][5] took the strain gradient elastic theory into the Bernoulli-Euler beam model. They analyzed the scale effect of bending, buckling and vibration of the beam. Further, Papargyri-Beskou and Beskos [6] derived the governing equations of Kirchhoff plates with strain gradient taken into account. They obtained analytic solutions for statics, dynamics and stability of simply supported plate.

All of above mentioned works deal with elastic structures with clamped boundary, free boundary or simply supported boundary, but elastic boundary condition is more practical. Jiang et al. [7] investigated the vibrational behaviors of single-walled carbon nanotubes bridged on a silicon channel using a three-segment Timoshenko beam model and a one-segment Timoshenko beam model with elastic boundaries together with molecular dynamics simulation. Li et al. [8] developed an analytical method for the vibration analysis of rectangular plates with elastic restrained edges. The displacement solution is expressed as a two-dimensional Fourier series with several supplemented series. Kiani [9] investigated the free transverse vibration of an elastically supported double-walled carbon nanotubes embedded in an elastic matrix under initial axial stress using reproducing kernel particle method.

The theoretical methods can only deal with the mechanical model of structures with simple boundary conditions. The finite element method (FEM), as an effective numerical tool, provides a feasible way to investigate complex nonlocal elastic structures with complex boundary condition . Engel et al. [10] presented a new continuous/discontinuous finite element method for fourth-order elliptic partial differential equations and applied it to structural of strain gradient elasticity. In order to study a strain gradient Kirchhoff plates with the van der Waals interactions, Xu et al. [11][12] proposed a 4-node 24-degree of freedom Kirchhoff plates element to discretize the sixth order partial differential equation with the small scale effect taken into consideration by the theory of virtual work. Soh and Chen [13] proposed the displacement function of the two kinds of elements based on the couple stress theory or the strain gradient theory. After Belytschko [14] putting forward the element free Galerkin method, various meshfree methods have been developed and applied to of static and dynamic problems of wide field. The meshfree method does not need girds, and the meshfree shape function has better continuity and smoothness. Furthermore the finite element method needs more degrees of freedom [11][12] at each node, whereas only one degree freedom is needed for one node in this paper using meshfree method when high-order partial differential equation of strain gradient theory is considered. Liu and Gu [15] proposed a point interpolation meshfree method based on combining radial and polynomial basis functions. The radial basis function overcomes possible singularity associated with the meshfree methods based on the polynomial basis. Liu et al. [16] presented an edge-based smoothed FEM (ES-FEM) to significantly improve the accuracy of the FEM without much changing to the standard FEM settings. The ES-FEM is applied in static, free and forced vibration analyses of solids. Liu [17][18] proposed a G space theory and a weakened weak form (W^2) using the generalized gradient smoothing technique for a unified formulation of a wide class of methods. The W^2 formulation works for both FEM settings and meshfree settings. W^2 models have special properties including softened behavior, upper bounds and ultra accuracy. Some applications of the G space theory to formulate W^2 models for solid mechanics problems were presented [18]. Wang et al.[19] studied the resonant frequencies and the associated vibration modes of an individual double-walled carbon nanotube, using gradient smoothing technique. Sun and Liew [20] developed a mesh-free method to deal with bending and buckling behaviors of single-walled carbon nanotubes. The results were compared with those obtained with a full atomistic simulation, and it revealed that the developed meshfree method can accurately simulate the bending deformation of single-walled carbon nanotubes. Xiang et al. [21] evaluated the influences of high-order terms on accuracy of the mechanical behaviors of microtubules. A specific meshless computational scheme based on third-order deformation gradient continuum was developed to suit the third-order Cauchy-Born rule for the mechanical simulation of microtubules. Yan et al. [22] investigated the free vibration characteristic of single-wall carbon nanocones by using a developed meshless computational framework based on moving Kriging interpolation. The proposed model can give a good prediction of the MD simulation and Timoshenko beam model. To the best knowledge of the authors, there is little work on the vibration of the strain gradient plates with elastic boundary conditions by using MLS method containing the higher order partial derivative of shape function.

The primary objective of this work is to investigate the vibration of the strain gradient plates with elastic boundary conditions. Next, the MLS method with a new shifted and scaled polynomial basis to approximate the field function are proposed in Section 2. Discretization of the governing equations for the strain gradient plates is presented in Section 3. The vibration characteristics of the strain gradient plates with elastic boundary condition are studied in Section 4. Finally, some concluding remarks are drawn in Section 5.

2. The moving least square (MLS) method

This section gives a brief summary of the MLS approximation scheme used in the following section. The approximate function $u^h(\mathbf{x})$ is constructed by MLS method. It can be expressed as

$$u^h(\mathbf{x}) = \sum_{i=1}^{q} p_i(\mathbf{x}) a_i(\mathbf{x}) = \mathbf{p}^{\mathrm{T}}(\mathbf{x})\mathbf{a}(\mathbf{x}) , \tag{1}$$

where $p_i(\mathbf{x})$ are the monomial basis function. A new shifted and scaled basis is used for constructing approximate function $u^h(\mathbf{x})$ [23][24]. In Equation (1), $a_i(\mathbf{x})$ is the corresponding coefficients, q is the number of the basic functions.

For two dimensional problems, the basic functions with 36 terms are as following

$$\begin{aligned}
\mathbf{p}^{\mathrm{T}} = [&1, \\
&\frac{x-x^e}{h}, \frac{y-y^e}{h}, \\
&\frac{(x-x^e)^2}{h^2}, \frac{(x-x^e)(y-y^e)}{h^2}, \frac{(y-y^e)^2}{h^2}, \\
&\frac{(x-x^e)^3}{h^5}, \frac{(x-x^e)^2(y-y^e)}{h^5}, \frac{(x-x^e)\,(y-y^e)^2}{h^5}, \frac{(y-y^e)^3}{h^5}, \\
&\frac{(x-x^e)^4}{h^5}, \frac{(x-x^e)^3(y-y^e)}{h^5}, \frac{(x-x^e)^2(y-y^e)^2}{h^5}, \frac{(x-x^e)^1(y-y^e)^3}{h^5}, \frac{(y-y^e)^4}{h^5}, \\
&\frac{(x-x^e)^5}{h^5}, \frac{(x-x^e)^4(y-y^e)}{h^5}, \frac{(x-x^e)^3(y-y^e)^2}{h^5}, \frac{(x-x^e)^2(y-y^e)^3}{h^5}, \frac{(x-x^e)^1(y-y^e)^4}{h^5}, \frac{(y-y^e)^5}{h^5}, \\
&\frac{(x-x^e)^5(y-y^e)}{h^6}, \frac{(x-x^e)^5(y-y^e)^2}{h^7}, \frac{(x-x^e)^5(y-y^e)^3}{h^8}, \frac{(x-x^e)^5(y-y^e)^4}{h^9}, \frac{(x-x^e)^5(y-y^e)^5}{h^{10}}, \\
&\frac{(x-x^e)^4(y-y^e)^2}{h^6}, \frac{(x-x^e)^4(y-y^e)^3}{h^7}, \frac{(x-x^e)^4(y-y^e)^4}{h^8}, \frac{(x-x^e)^4(y-y^e)^5}{h^9}, \\
&\frac{(x-x^e)^3(y-y^e)^3}{h^6}, \frac{(x-x^e)^3(y-y^e)^4}{h^7}, \frac{(x-x^e)^3(y-y^e)^5}{h^8}, \\
&\frac{(x-x^e)^2(y-y^e)^4}{h^6}, \frac{(x-x^e)^2(y-y^e)^5}{h^7}, \\
&\frac{(x-x^e)(y-y^e)^5}{h^6}].
\end{aligned} \tag{2}$$

For $\mathbf{x}^e = \left(x^e, y^e\right)$, $\mathbf{x}^e$ is specified to be Gauss point. In Equation (2), h is defined as [23]

$$h = \max_{1\le I\le N} \min_{1\le J\le N, J\ne I} \left|\mathbf{x}_I - \mathbf{x}_J\right| . \tag{3}$$

The weighted discrete L^2 norm is given as

$$J = \sum_{I=1}^{N} \overline{w}(\mathbf{x}-\mathbf{x}_I)[\mathbf{p}^{\mathrm{T}}(\mathbf{x})\mathbf{a}(\mathbf{x}) - u_I]^2 , \tag{4}$$

where a new weight function $\overline{w}(\mathbf{r})$ is given as

$$\overline{w}(r_I) = \begin{cases} 1-126r_I^5 + 420r_I^6 - 540r_I^7 + 315r_I^8 - 70r_I^9 & 0 \le r_I \le 1, \\ 0 & r_I \ge 1. \end{cases} \tag{5}$$

where the normalized distance r_I is defined as

$$r_I = \frac{\left\|\mathbf{x}-\mathbf{x}_I\right\|}{d_I} , \tag{6}$$

with d_I being the size of the support domain of node *I*. For a rectangular support, d_I can be denoted as

$$\mathrm{d}x_I = d_{\max} \cdot \mathrm{d}x_{bI} , \quad \mathrm{d}y_I = d_{\max} \cdot \mathrm{d}y_{bI} , \tag{7}$$

where $\mathrm{d}x_{bI}$ and $\mathrm{d}y_{bI}$ refer to the distances between two adjacent nodes along x and y directions, respectively, and $d_{\max}$ denotes the scaling factor.

After the minimization of the weighted discrete L2 norm with respect to $\mathbf{a}(\mathbf{x})$, it can be expressed as

$$\mathbf{a}(\mathbf{x}) = \mathbf{A}^{-1}(\mathbf{x})\mathbf{B}(\mathbf{x})\mathbf{u} . \tag{8}$$

Substituting Equation (8) into Equation (1), the expression of approximation $u^h(\mathbf{x})$ is given by

$$u^h(\mathbf{x}) = \sum_{I=1}^{n} \phi_I(\mathbf{x}) u_I , \tag{9}$$

where the shape function is given as[25]

$$\phi_I(\mathbf{x}) = \overline{w}(\mathbf{x} - \mathbf{x}_\mathrm{I})\mathbf{p}^\mathrm{T}(\mathbf{x})\mathbf{A}(\mathbf{x})\mathbf{P}(\mathbf{x}_\mathrm{I}) . \tag{10}$$

The above shape function can be used to deal with the vibration problems of the strain gradient plates.

3. Discretization of the governing equations for strain gradient plates

Here a square plate made of strain gradient material with elastic boundary containing translational and rotational spring is considered, as shown in Figure 1.

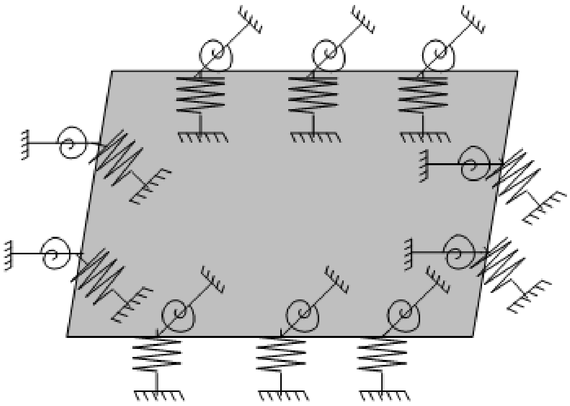

Figure 1. A square plate with elastic boundary

The constitute relation of the strain gradient theory is given as [26]

$$\boldsymbol{\sigma} = \mathbf{H}\left(\boldsymbol{\varepsilon} + g^2 \nabla^2 \boldsymbol{\varepsilon}\right), \tag{11}$$

where $\boldsymbol{\sigma}$ and $\boldsymbol{\varepsilon}$ are the stress and strain vectors, respectively, g is the intrinsic scale parameter to capture the size effect, $\nabla^2 = \partial^2/\partial x^2 + \partial^2/\partial y^2$ denotes the Laplacian operator. For plane stress problem H is given as

$$\mathbf{H} = \frac{E}{1-\mu^2}\begin{bmatrix} 1 & \mu & 0 \\ \mu & 1 & 0 \\ 0 & 0 & \frac{1-\mu}{2} \end{bmatrix}, \tag{12}$$

where μ is the Poisson ratio.

According to theory of Kirchhoff plate, the strain of the plate can be written as

$$\varepsilon_x = -z\frac{\partial^2 w}{\partial x^2}, \varepsilon_y = -z\frac{\partial^2 w}{\partial y^2}, \gamma_{xy} = 2\varepsilon_{xy} = -2z\frac{\partial^2 w}{\partial xy} . \tag{13}$$

Substituting Equation (12) and (13) into Equation (11) results in

$$\begin{cases} \sigma_{xx} = \dfrac{E}{1-\mu^2}\left(-z\dfrac{\partial^2 w}{\partial x^2} - \mu z\dfrac{\partial^2 w}{\partial y^2}\right) + g^2\dfrac{E}{1-\mu^2}\nabla^2\left(-z\dfrac{\partial^2 w}{\partial x^2} - \mu z\dfrac{\partial^2 w}{\partial y^2}\right), \\ \sigma_{yy} = \dfrac{E}{1-\mu^2}\left(-z\dfrac{\partial^2 w}{\partial y^2} - \mu z\dfrac{\partial^2 w}{\partial x^2}\right) + g^2\dfrac{E}{1-\mu^2}\nabla^2\left(-z\dfrac{\partial^2 w}{\partial y^2} - \mu z\dfrac{\partial^2 w}{\partial x^2}\right), \\ \tau_{xy} = \dfrac{E}{1+\mu}\left(-z\dfrac{\partial^2 w}{\partial x\partial y}\right) + g^2\dfrac{E}{1+\mu}\nabla^2\left(-z\dfrac{\partial^2 w}{\partial x\partial y}\right). \end{cases} \tag{14}$$

So the strain energy of the plate can be given as

$$V_p = \iiint_V \left(\sigma_x\delta\varepsilon_x + \sigma_y\delta\varepsilon_y + \tau_{xy}\delta\gamma_{xy}\right)\mathrm{d}V \,. \tag{15}$$

The displacement function is assumed as

$$w(x,y,t) = W(x,y)e^{j\omega t}\,, \tag{16}$$

where $W(x,y)$ is the mode function, ω is the natural frequency and $j \equiv \sqrt{-1}$.

The kinetic energy of rectangular plate can be expressed as

$$T = \frac{1}{2}\rho h\omega^2 \iint w^2 \mathrm{d}x\mathrm{d}y\,. \tag{17}$$

The potential energy of elastic boundary containing translational spring and rotational spring is

$$V_s = \frac{1}{2}\int_{\Gamma_k} kw^2\mathrm{d}\Gamma_k + \frac{1}{2}\int_{\Gamma_K} K\theta^2\mathrm{d}\Gamma_K\,. \tag{18}$$

where k and K are translational spring stiffness and rotational spring stiffness, respectively. Γ_k and Γ_K are the boundary with linear translational spring and rotational spring, respectively.

The energy of the transverse vibration of the plates ignoring body force and surface force can be given as

$$\Pi = \int_\Omega \left(T - V_p - V_s\right)\mathrm{d}V\,. \tag{19}$$

The penalty function method is used to deal with the simple supported and clamped boundary conditions. So, according to Hamilton principle, one can get

$$\delta\left(\Pi + \frac{1}{2}\alpha_1\int_{\Gamma_1}\left(w-\overline{w}\right)^2\mathrm{d}\Gamma_1 + \frac{1}{2}\alpha_2\int_{\Gamma_2}\left(\theta-\overline{\theta}\right)^2\mathrm{d}\Gamma_2\right) = 0\,, \tag{20}$$

where α_1 α_2 are penalty coefficient of linear displacement and angular displacement, respectively. In this paper $\alpha_1 = \alpha_2 = 1.0\times10^4 E$ is used. $\overline{w}$ and $\overline{\theta}$ are the given linear displacement and angular displacement, respectively.

Inserting Equation (19) into Equation (20), one can get

$$\begin{aligned} &\iiint_V\left(\sigma_x\delta\varepsilon_x + \sigma_y\delta\varepsilon_y + \tau_{xy}\delta\gamma_{xy}\right)\mathrm{d}V + \frac{1}{2}\delta\int_{\Gamma_k} kw^2\mathrm{d}\Gamma_k + \frac{1}{2}\delta\int_{\Gamma_K} K\theta^2\mathrm{d}\Gamma_K \\ &+\frac{1}{2}\alpha_1\delta\int_{\Gamma_1}\left(w-\overline{w}\right)^2\mathrm{d}\Gamma_1 + \frac{1}{2}\alpha_2\delta\int_{\Gamma_2}\left(\theta-\overline{\theta}\right)^2\mathrm{d}\Gamma_2 - \frac{1}{2}\rho h\omega^2\delta\iint w^2\mathrm{d}x\mathrm{d}y = 0 \end{aligned}\,. \tag{21}$$

Integrating the forth order partial derivative by part, then using the Stokes formula, then The first term of Equation (21) is given as

$$V_p = \iiint_V \left(\sigma_x \delta\varepsilon_x + \sigma_y \delta\varepsilon_y + \tau_{xy}\delta\gamma_{xy}\right)\mathrm{d}V$$

$$= D_0 \iint \left\{ \begin{array}{l} \left[\left(w_{xx} + \mu w_{yy}\right)\delta w_{xx} + \left(w_{yy} + \mu w_{xx}\right)\delta w_{yy} + 2(1-\mu) w_{xy}\delta w_{xy}\right] \\ -g^2\left[\left(w_{xxx} + \mu w_{xyy}\right)\delta w_{xxx} + \left(w_{xyy} + \mu w_{xxx}\right)\delta w_{xyy} + 2(1-\mu) w_{xxy}\delta w_{xxy}\right] \\ -g^2\left[\left[\left(w_{yyy} + \mu w_{xxy}\right)\delta w_{yyy} + \left(w_{xxy} + \mu w_{yyy}\right)\delta w_{xxy} + 2(1-\mu) w_{xyy}\delta w_{xyy}\right]\right] \end{array} \right\} \mathrm{d}x\mathrm{d}y \tag{22}$$

$$+ g^2 D_0 \oint_\Gamma \left\{ \begin{array}{l} \left[w_{xxx}\delta w_{xx} + \mu w_{xyy}\delta w_{xx} + w_{xyy}\delta w_{yy} + \mu w_{xxx}\delta w_{yy} + 2(1-\mu) w_{xxy}\delta w_{xy}\right]\mathrm{d}y \\ -\left[w_{yyy}\delta w_{yy} + \mu w_{xxy}\delta w_{yy} + w_{xxy}\delta w_{xx} + \mu w_{yyy}\delta w_{xx} + 2(1-\mu) w_{xyy}\delta w_{xy}\right]\mathrm{d}x \end{array} \right\}$$

where D_0 is bending stiffness: $D_0 = Eh^3 / 12\left(1-\mu^2\right)$.

According to MLS method, one can get

$$w = \sum_{I=1}^{NP} \phi_I w_I \ , \ w_{,k} = \sum_{I=1}^{NP} \phi_{I,k}(x) w_I \ , \ w_{,kl} = \sum_{I=1}^{NP} \phi_{I,kl}(x) w_I \ , \ w_{,klf} = \sum_{I=1}^{NP} \phi_{I,klf}(x) w_I \ . \tag{23}$$

where $w_{,k}$, $w_{,kl}$, $w_{,klf}$ refer to the first the second and the third order partial derivatives of w, respectively, and k, l, f mean x or y.

Substituting Equation (17), (18), (22) into Equation (20), Then inserting Equation (23) into Equation (20), one can get

$$\mathbf{K} - \omega^2 \mathbf{M} = \mathbf{0} \ . \tag{24}$$

where $\mathbf{K}$ is the global stiffness matrix, $\mathbf{M}$ is the global mass matrix.

Furthermore, $\mathbf{K}$ can be expressed by another form

$$\mathbf{K} = \mathbf{K}^p + \mathbf{K}^s + \mathbf{K}^\alpha \ . \tag{25}$$

where $\mathbf{K}^p$ is assembled by nodal stiffness, which is defined as

$$K_{IJ}^p = \iint \left(\mathbf{C}_I^\mathbf{T}\mathbf{D}\mathbf{C}_J - g^2 \frac{\partial}{\partial x}\left(\mathbf{C}_I^\mathbf{T}\right)\mathbf{D}\frac{\partial}{\partial x}\left(\mathbf{C}_J\right) - g^2 \frac{\partial}{\partial y}\left(\mathbf{C}_I^\mathbf{T}\right)\mathbf{D}\frac{\partial}{\partial y}\left(\mathbf{C}_J\right) \right)\mathrm{d}x\mathrm{d}y$$
$$+ \oint g^2 \frac{\partial}{\partial x}\left(\mathbf{C}_I^\mathbf{T}\right)\mathbf{D}\mathbf{C}_J\mathrm{d}y - \oint g^2 \frac{\partial}{\partial y}\left(\mathbf{C}_I^\mathbf{T}\right)\mathbf{D}\mathbf{C}_J\mathrm{d}x \ , \tag{26}$$

where $\mathbf{C}_I$ and $\mathbf{D}$ are define as

$$\mathbf{C}_I = [\phi_{I,xx}, \phi_{I,yy}, 2\phi_{I,xy}]^\mathbf{T} \ , \tag{27}$$

$$\mathbf{D} = D_0 \begin{bmatrix} 1 & v & 0 \\ v & 1 & 0 \\ 0 & 0 & \dfrac{(1-v)}{2} \end{bmatrix} , \tag{28}$$

where $\mathbf{K}^s$ is assembled by

$$K_{IJ}^s = \int_{\Gamma_k} k \phi_I \phi_J \mathrm{d}\Gamma_k + \int_{\Gamma_K} K \phi_{I,} \phi_{J,} \mathrm{d}\Gamma_K \ . \tag{29}$$

For the case of $\bar{w} = 0$ and $\bar{\theta} = 0$, the element of the $\mathbf{K}^\alpha$ for the displacement boundary condition can be given as

$$K_{IJ}^\alpha = \int_{\Gamma_1} \alpha_1 \phi_I \phi_J \mathrm{d}\Gamma_1 + \int_{\Gamma_2} \alpha_2 \phi_{I,} \phi_{J,} \mathrm{d}\Gamma_2 \ . \tag{30}$$

So the element of stiffness matrix of the strain gradient plates with elastic boundary is

$$K_{IJ} = K_{IJ}^p + K_{IJ}^s + K_{IJ}^\alpha \ . \tag{31}$$

In Equation (24), the $\mathbf{M}$ is assembled by

$$M_{IJ} = \rho h \iint_S \phi_I \phi_J \mathrm{d}x\mathrm{d}y \ . \tag{32}$$

So, the natural frequency of the strain gradient plates can be calculated.

4. Vibration of the strain gradient plates with elastic boundary conditions

In this section, a square nanoplate with side length $a = b = 5\,\text{nm}$ and thickness h=0.11nm is considered. The Young's Modulus of the plate is E=2.28TPa, the Possion's ratio v=0.41, the density $\rho = 7.016 \times 10^3\, kg/m^3$, the scale parameter g=0.0355nm. The scaling factor $d_{\max} = 6$ is adopted in this paper.

In order to verify the applicability of the MLS method to solve the strain gradient nanoplate with simply supported boundary, the natural frequencies of the square strain gradient plate are presented in Figure 2. It can be seen that the meshless solution is in good agreement with exact solution in Figure 2 (a). Frequency ratio of the meshless solution is in good agreement with exact solution, as show in Figure 2 (b). The natural frequencies of the strain gradient plate with simply supported boundary is given as [11][12]

$$\omega = \pi^2 \sqrt{\frac{D}{\rho h}} \left(\frac{m^2}{a^2} + \frac{n^2}{b^2} \right) \sqrt{1 - g^2 \pi^2 \left(\frac{m^2}{a^2} + \frac{n^2}{b^2} \right)} \quad (m, n = 1,2,3), \tag{33}$$

where a, b are length and width , respectively, and m, n are half-wave number along x axis and y axis, respectively.

The strain gradient plate will be degenerated into the classic Kirchhoff plate, when the intrinsic scale parameter g=0. The natural frequencies of classical simply supported Kirchhoff plate can be expressed as

$$\varpi = \pi^2 \sqrt{\frac{D}{\rho h}} \left(\frac{m^2}{a^2} + \frac{n^2}{b^2} \right) \quad (m, n = 1,2,3), \tag{35}$$

The frequency ratio of the strain gradient plate to the classical Kirchhoff plate can be expressed as

$$\frac{\omega}{\varpi} = \sqrt{1 - g^2 \pi^2 \left(\frac{m^2}{a^2} + \frac{n^2}{b^2} \right)} \quad (m, n = 1,2,3), \tag{36}$$

These proves the applicability of MLS in solving the strain gradient plate with simple supported boundary condition.

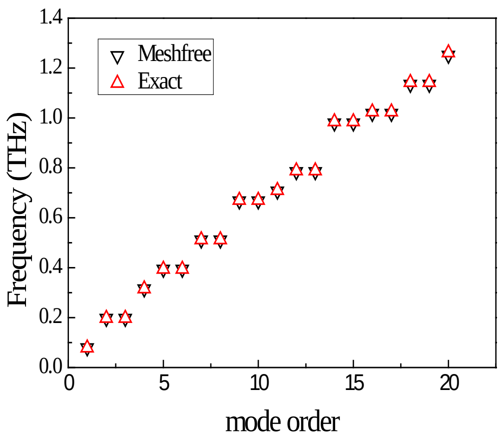

(a)

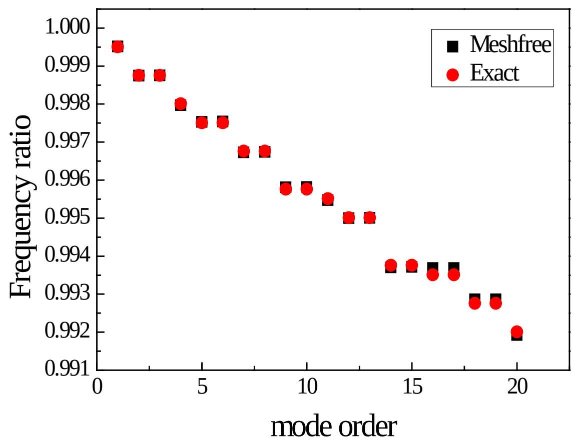

(b)

Figure 2. The natural frequency and the frequency ratio using meshfree methd and analytic method. (a) Natural frequency of the strain gradient plate via MLS method compared with Exact solution (b) Frequency ratio for the strain gradient plate via MLS method compared with Exact solution.

Figure 3 present the first order frequency of the 5nm×5nm nanoplate with different scale parameters. Here 41×41 nodes are used and g=0.0355nm. It can be seen that the meshless result and exact result match reasonably well for most case. But the different of natual frequencies at point 0.9g and 1.2g is obviously. Nevertheless the meshless result is very close to the exact, because the maximum error are 0.222‰ at the point 0.9g *and* 0.569‰ at the point 1.2g.

The natural frequency of the simply supported classic Kirchhoff plates with uniform rotational restraint along edges is presented in Table 1. The translational degree of freedom of all boundaries fixed. It can be easily seen from Table 1 that these three sets of results match very well with each other. It shows the applicability of MLS in solving plate with elastic boundary.

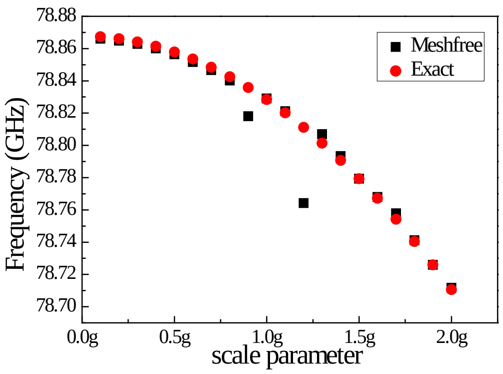

Figure 3. The first order frequency of nanoplate with different scale parameters

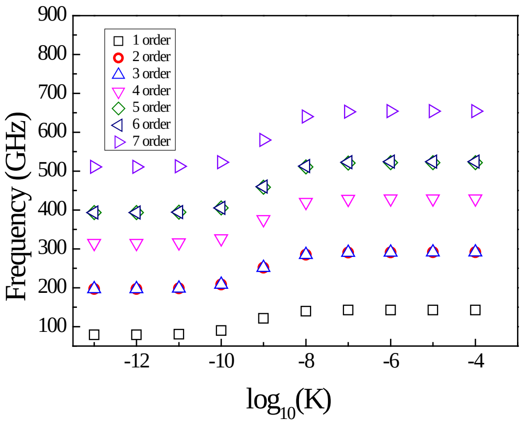

Figure 4. The first seven natural frequency of the nanoplate

Table 1. Natural frequency parameter of the classic Kirchhoff plates with uniform rotational restraint along edges.

Ka/D	$\Omega=\omega^2\sqrt{\rho h/D}$					
	1	2	3	4	5	6
1	21.502	51.189	51.189	80.822	100.567	100.574
	21.500a	51.187	51.187	80.816	100.58	100.58
	21.496b	51.184	51.187	80.818	100.58	100.58
10	28.496	60.211	60.211	90.811	111.181	111.402
	28.501a	60.215	60.215	90.808	111.19	111.41
	28.489b	60.196	60.196	90.79	111.16	111.39
100	34.649	70.751	70.751	104.42	126.98	127.565
	34.671a	70.78	70.78	104.45	127.02	127.61
	34.668b	70.771	70.78	104.44	127.01	127.59
1000	35.817	73.065	73.065	107.748	131.007	131.625
	35.842a	73.103	73.103	107.79	131.06	131.68
	35.842b	73.100	73.100	107.78	131.06	131.68

[a]Results from Ref. [8],
[b]Results form FEM with 300×300 elements [8].

Figure 4 presents the first seven natural frequencies of the strain gradient nanoplate 5nm×5nm g=0.0355nm with 51×51 nodes. The unit of the translational spring k and the rotational spring K are N/m^2, N, respectively. The first seven order frequency has the same trend. Figure 4. shows that frequency will increase if K increases. There exist significant growth during $\log_{10} K \in [-11,-8]$) .

Figure 5 shows the natural frequency of the 5nm×5nm nanoplate with g=0.0355nm using 51×51 nodes. Both Figure 5. (a) and Figure 5. (b) show us that the the natural frequency of the strain gradient plateis very close to that of the classic Kirchhoff plate. And the frequency will increase with the increasing of translational spring stiffness k and rotational spring stiffness K. There exists significant growth interval ($\log_{10} k \in [6,10]$) of k. And there exist significant growth during $\log_{10} K \in [-11,-8]$) also.

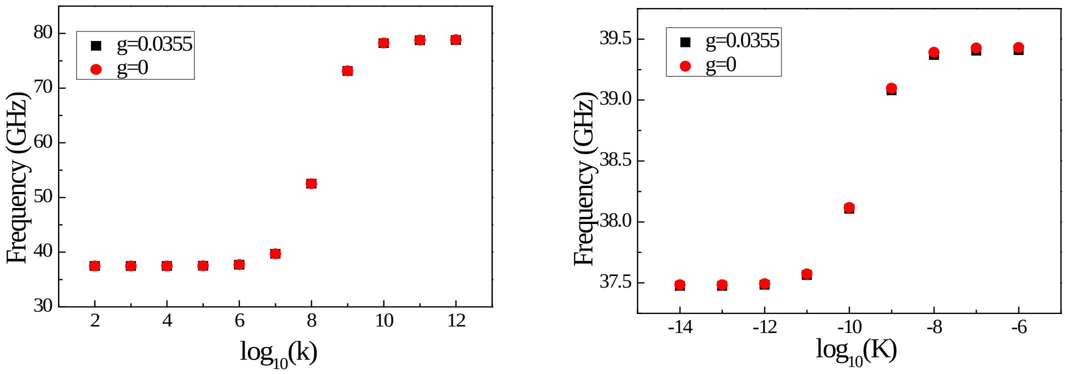

(a) **(b)**

Figure 5. Natural frequency of the 5nm×5nm nanoplate with g=0.0355nm with 51×51 nodes. (a) Frequency for nanoplate of two opposite edges simply supported and the others are supported by translational spring. (b) Frequency for nanoplate of two opposite edges simply supported and the others are supported by rotational spring.

5. Conclusions

A the MLS method with high-order shifted and scaled polynomial basis is proposed to study the vibration of strain gradient plate. Several numerical examples are presented to demonstrate the accuracy of MLS method with high-order shifted and scaled polynomial basis. The vibration of strain gradient plate with elastic boundary condition is studied. Numerical results of the meshfree method are in good agreement with analytic solutions and the results in the related literature. This method may also be extended to other more complex boundary condition such as non-uniform elastic restraints.

Acknowledgments

This work was supported in part by the National Natural Science Foundation of China under Grants 11522217.

Reference

[1] Toupin, R. A. (1962) Elastic materials with couple-stresses. *Archive for Rational Mechanics and Analysis* **11**, 385-414.

[2] Mindlin, R. D., (1962) Tiersten, H. F. Effects of couple-stresses in linear elasticity. *Archive for Rational Mechanics and Analysis* **11**, 415-448.

[3] Mindlin, R. D. (1964) Micro-structure in linear elasticity. Archive for Rational Mechanics and Analysis **16**, 51-78.

[4] Papargyri-Beskou, S., Tsepoura, K. G., Polyzos, D., Beskos D.E. (2003) Bending and stability analysis of gradient elastic beams. International Journal of Solids and Structures **40**, 385-400.
[5] Papargyri-Beskou, S., Polyzos, D., Beskos, D. E. (2003) Dynamic analysis of gradient elastic flexural beams. *Structural Engineering and Mechanics* **15**, 705-716.
[6] Papargyri-Beskou, S., Beskos, D. E. (2008) Static, stability and dynamic analysis of gradient elastic flexural Kirchhoff plates. *Archive of Applied Mechanics* **78**, 625-635.
[7] Jiang, J. N., Wang, L. F., Zhang, Y. Q. (2017) Vibration of Single-Walled Carbon Nanotubes with Elastic Boundary Conditions. *International Journal of Mechanical Sciences* **122**, 156-166.
[8] Li, W. L., Zhang, X., Du, J., Liu, Z. (2009) An exact series solution for the transverse vibration of rectangular plates with general elastic boundary supports. *Journal of Sound and Vibration* **321**, 254-269.
[9] Kiani, K. (2013) Vibration analysis of elastically restrained double-walled carbon nanotubes on elastic foundation subjected to axial load using nonlocal shear deformable beam theories. *International Journal of Mechanical Sciences* **68**, 16-34.
[10] Engel, G., Garikipati, K., Hughes, T. J. R., Larson, M. G., Mazzei, L. and Taylor, R. L. (2002) Continuous/discontinuous finite element approximations of fourth-order elliptic problems in structural and continuum mechanics with applications to thin beams and plates, and strain gradient elasticity. *Computer Methods in Applied Mechanics and Engineering* **191**, 3669-3750.
[11] Xu, W., Wang, L. F., Jiang J. N. (2014) Finite element analysis of strain gradient on the vibration of single-layered graphene sheets. *Chinese Journal of Solid Mechanics* **35**, 441-450.
[12] Xu, W., Wang, L. F., Jiang, J. N. (2016) Strain Gradient Finite Element Analysis on the Vibration of Double-Layered Graphene Sheets. *International Journal of Computational Methods* **13**, 1650011.
[13] Soh, A. K., Chen, W. J. (2004) Finite element formulations of strain gradient theory for microstructures and the C0–1 patch test. *International Journal for Numerical Methods in Engineering* **61**, 433-454.
[14] Belytschko, T., Lu, Y. Y., Gu, L. (1994) Element ‐ free Galerkin methods. *International Journal for Numerical Methods in Engineering* **37**, 229-256.
[15] Liu, G. R., Gu, Y. T. (2001) A local radial point interpolation method (LRPIM) for free vibration analyses of 2-D solids. *Journal of Sound and Vibration* **246**, 29-46.
[16] Liu, G. R., Nguyen-Thoi, T., Lam, K. Y. (2009) An edge-based smoothed finite element method (ES-FEM) for static, free and forced vibration analyses of solids. *Journal of Sound and Vibration* **320**, 1100-1130.
[17] Liu, G. R. (2010a). AG space theory and a weakened weak (W^2) form for a unified formulation of compatible and incompatible methods: Part I theory. *International Journal for Numerical Methods in Engineering* **81**, 1093-1126.
[18] Liu, G. R. (2010b). AG space theory and a weakened weak (W^2) form for a unified formulation of compatible and incompatible methods: Part II applications to solid mechanics problems. *International Journal for Numerical Methods in Engineering* **81**, 1127.
[19] Wang, L. F., Han, D., Liu, G. R., and Cui, X. Y. (2011). Free vibration analysis of double-walled carbon nanotubes using the smoothed finite element method.International Journal of Computational Methods **8**, 879-890.
[20] Sun, Y. Z., Liew, K. M. (2008) The buckling of single-walled carbon nanotubes upon bending: the higher order gradient continuum and mesh-free method. Computer Methods in Applied Mechanics and Engineering **197**, 3001-3013.
[21] Xiang, P., Zhang, L. W., Liew, K. M. (2017) A third-order Cauchy-Born rule for modeling of microtubules based on the element-free framework. *Composite Structures* **161**, 215-226.
[22] Yan, J. W., Zhang, L. W., Liew, K. M., He, L. H. (2014) A higher-order gradient theory for modeling of the vibration behavior of single-wall carbon nanocones. *Applied Mathematical Modelling* **38**, 2946-2960.
[23] Li, X. L., Li, S. L. (2016) On the stability of the moving least squares approximation and the element-free Galerkin method. *Computers & Mathematics with Applications* **72**, 1515-1531.
[24] Li, X. L., Wang, Q. Q. (2016) Analysis of the inherent instability of the interpolating moving least squares method when using improper polynomial bases. *Engineering Analysis with Boundary Elements* **73**, 21-34.
[25 Liu, G. R., Gu, Y. T. (2005) An introduction to meshfree methods and their programming. Springer Science & Business Media, 80-100.
[26] Askes, H., Suiker, A. S. J., Sluys, L. J. (2002) A classification of higher-order strain-gradient models–linear analysis. *Archive of Applied Mechanics* **72**, 171-188.

Biography

Lifeng Wang received his Ph.D. from Nanjing University of Aeronautics and Astronautics, China, in 2005. He was a Research Fellow at the Centre for Advanced Computations in Engineering Science (ACES), National University of Singapore for three months in 2009. He is currently a Professor at College of Aerospace Engineering in Nanjing University of

Aeronautics and Astronautics. His research interests focus on dynamics problems in advanced structures. He have authored 40 journal papers. He was granted the Fund for Excellent Youth Researchers from NSFC in 2015. He is the recipient of numerous awards, the Excellent Doctoral Dissertation Award of China in 2009, the Second Prize of National Natural Science Award of China(Achiever No.5) in 2012, The Young Chang Jiang Scholars Programme in 2015.